Journal of Naval Sciences and Engineering
2021, Vol. 17, No. 1, pp. 27-42
Electric-Electronic Engineering/Elektrik-Elektronik Mühendisliği

RESEARCH ARTICLE

**An ethical committee approval and/or legal/special permission has not been required within the scope of this study.*

A NOVEL TENSOR RPCA METHOD FOR CLUTTER SUPPRESSION IN GPR IMAGES*

Deniz KUMLU[1]
Batuhan GÜNDOĞDU[2]

[1]Navy Research Center, Turkish Naval Forces, Istanbul, Turkey, dkumlu@gmail.com; ORCID: 0000-0002-7192-7466

[2]National Defence University, Turkish Naval Academy, Department of Electrical and Electronics Engineering, Istanbul, Turkey, mbgundogdu@dho.edu.tr; ORCID: 0000-0002-9395-7519

Received: 07.10.2020 **Accepted: 21.01.2021**

ABSTRACT

The clutter problem in ground penetrating radar (GPR) images highly effects the peformance of target detection ratio. Various methods have been proposed for clutter suppression purposes in the GPR literature. They can be mainly grouped as low rank, low rank and sparse and tensor-based decomposition methods. Principal component analysis (PCA) and robust principal component analysis (RPCA) are classicle approaches and could be classified as low rank and low rank/sparse decomposition methods, respectively. Recently proposed tensor-based methods provide an alternative perspective of solving the low rank and sparse decomposition to handle challenging situations such as shallowly buried objects or rough surface situations. Motivated by the performance of Tensor-based methods, we propose a new pre-transformation step for tensor robust principal component analysis (TRPCA) and compare it with the PCA and RPCA methods over a simulated GPR dataset. Our proposed method outperforms the classical PCA and recent RPCA methods both visually and quantitatively in terms of clutter removal.

Keywords: *Ground Penetrating Radar (GPR), Principal Component Analysis (PCA), Robust PCA (RPCA), Tensor RPCA (TRPCA), gprMax.*

YNR GÖRÜNTÜLERİNDE KARGAŞANIN BASTIRILMASI İÇİN ÖZGÜN TENSÖR GTBA METODU

ÖZ

Yere nüfuz eden radar (YNR) görüntülerinde kargaşanın varlığı hedef tespit oranını büyük ölçüde etkilemektedir ve kargaşanın bastırılması için birçok yöntem önerilmiştir. Bu yöntemler temel olarak alçak sıra, alçak sıra ve seyrek ve tensör ayrıştırma yöntemleri olarak gruplanabilir. Temel bileşen analizi (TBA) kargaşa bastırma yöntemler arasında ilk akla gelen yöntemdir ve alçak sıra ailesinde yer alır. Daha sonra, bu yöntem alçak sıra ve seyrek ayrıştırma yöntemi olarak gürbüz temel bileşen analizi (GTBA) adıyla geliştirilmiş ve yüzeye yakın gömülen hedefler ve pürüzlü yüzeyler gibi zorlu durumlarla başa çıkabilir hale gelmiştir. Son zamanlarda önerilen tensör tabanlı yöntemler alçak sıra ve seyrek ayrıştırma problemine alternatif çözümler sağlamaktadır. Bu yöntemlerin sonuçlarından motive olarak, yeni bir ön-dönüşüm adımı ile tensör gürbüz temel bileşen analizi (TGTBA) yöntemi önerilmiştir ve önerilen yöntem TBA ve GTBA yöntemleri ile benzetim veri seti üzerinden karşılaştırılmıştır. Önerdiğimiz yöntem klasik TBA ve yeni önerilen GTBA yöntemlerine karşı hem görsel hem de sayısal olarak üstünlük sağlamıştır.

Anahtar Kelimeler: *Yere Nüfuz Eden Radar (YNR), Temel Bileşen Analizi (TBA), Gürbüz TBA (GTBA), Tensör GTBA (TGTBA), gprMax.*

1. INTRODUCTION

Ground-penetrating radar (GPR) is an effective and nondestructive geophysical tool for near surface applications and it is widely used for buried object detection. GPR sends radar pulses and uses the electromagnetic properties of the penetrated materials (dielectric permittivity, electrical conductivity and magnetic permeability) to image the subsurface. The received signal in one iteration constitutes the A-scan which is a 1D signal and concatenation of A-scans constitutes the B-scan or GPR image (Daniels, 2005).

The major problem in the obtained GPR image is that the target signature is obscured by the clutter. The clutter can be arisen from several reasons such as ground-bounce, direct-wave arrival, presence of other candidate objects and environmental factors. To increase the detection probability, the clutter effect has to be suppressed. For this purpose, various methods are proposed and we can divide them into 4 major groups as low rank decomposition based methods (Verma et al., 2009), multi-resolution based methods (Kumlu & Erer, 2018; Kumlu, Erer, & Kaplan, 2020b), low rank and sparse decomposition based methods (Tivive, Bouzerdoum, & Abeynayake, 2019; Kumlu & Erer, 2020a) and tensor decomposition based methods (Song et al., 2019). The first three groups are widely studied in the literature (Verma et al., 2009; Kumlu & Erer, 2018; Kumlu & Erer, 2020a) and many methods are proposed. The latest one (Song et al., 2019) is a new subject and it is now trending topic.

The most popular method for clutter removal is principal component analysis (PCA) which belongs to low rank based methods (Abujarad & Omar, 2006). It is used to decompose GPR image into many sub-images which equal to the number of A-scans. The sub-image belongs to the most significant eigenvector corresponds to the clutter component and the sum of remaining sub-images constitute the target component. The main problem of PCA is that it cannot remove clutter well enough if the target is shallowly buried or the surface of the ground is rough.

The robust principal component analysis (RPCA) is a low rank and sparse decomposition based method (Song et al., 2017). It exploits the low rank property of clutter and sparse property of target. After the decomposition by RPCA, the obtained low rank part corresponds to clutter component and the sparse part corresponds to target component. It shows superior performance compared to the classical PCA method however it still have some trouble during shallowly buried objects and rough surfaces.

The tensor robust principal component analysis (TRPCA) is recently proposed in GPR image decomposition (Song et al., 2019) and it exploits the advantage of multidimensional tensor and provides an alternative perspective of solving the low rank and sparse decomposition problem. In (Song et al., 2019), they are using low and high frequency filtering results of the GPR image to create an image tensor. The aim is to contain the spatial characteristics and spectral information during the GPR image decomposition. In our proposed method, we divide the GPR image into patches thus image-patch tensor is constructed. Each patch corresponds to the related A-scan and it keeps the structural information as patch-image. This procedure is a pre-transformation step. Then, TRPCA method is used and it effectively decomposes to GPR image into its clutter and target component.

The rest of the paper is organized as follows. Section 2 introduces a methodology for GPR clutter suppression method. Results for simulated datasets as well as comparisons with PCA and RPCA are presented in section 3. Concluding remarks are given in section 4.

2. METHODOLOGY

PCA is the traditional matrix decomposition method and it is extensively used for clutter suppression in GPR. The GPR image is a two dimensional matrix denoted by $X \in R^{M \times N}$ where M and N represent the time and distance index, respectively. PCA decomposes X into sum of low rank component L and noise component N, i.e., $X = L + N$. The PCA method searches for the best rank-k estimate of X by minimizing the following cost function (Wold, Esbensen & Geladi, 1987).

$$\min_L \|X - N\|_F^2 \quad \text{s.t.} \quad \text{rank}(L) \le k \qquad \textbf{(1)}$$

Here *F* refers to Frobenius norm. For the decomposition subspace, the most dominant component (the highest eigenvalue) equals to the clutter image and sum of the rest equals to target image in practical.

However, the well-known PCA method cannot efficiently decompose the GPR image if there is severe clutter present which generally corresponds to the field data. To overcome this drawback, the robust version of PCA is proposed which is called as RPCA.

The aim of the RPCA method is to find a low rank approximation as well a sparse approximation (Candès et. al, 2011) of the GPR image X where the low rank component denotes L, and the sparse component denotes S. Thus, the cost function of RPCA is

$$min_{L,S} \|L\|_* + \lambda \|S\|_1 \quad \text{s.t.} \quad X = L + S \qquad \textbf{(2)}$$

Where$\|L\|_*$, $\|S\|_1$, and λ denote the matrix nuclear norm of L, L1-norm of S and the regularization term, respectively. The main motivation of the cost function in (2) is the nuclear norm and L1-norm provides the tightest convex relaxation for the rank of input matrix and L0-norm.

RPCA method shows superior performance compared to the classical PCA method, however, it still has some trouble for the severe clutter case. In the literature, the tensor based methods are proposed to provide an alternative solution for the low rank and sparse decomposition for multi-dimensional data and it exploits the information where contained in different dimensions. Tensor RPCA or known as TRPCA which is effectively applied to video processing, seismic denoising, and target detection problems (Lu et al., 2019).

To apply TRPCA, the pre-transformation step is necessary for GPR image which is the novelty of our work. In order to construct the multi-dimensional data, we divide the GPR image into $r \times r$ patches. As a result, the GPR image $X \epsilon R^{M \times N}$ is converted into $D \in R^{r \times r \times N}$ to construct the image-patch tensor. In our problem, the parameter *r* is selected as $\sqrt{M}$ since the length of the A-scans are equaled to *M*. Thus, the relation between each A-scans are modeled as image-patch tensor and A-scans are converted to 2D form by reshaping column vector with length M into $\sqrt{M} \times \sqrt{M}$ image.

The cost function for TRPCA is

$$min_{L,S}\|L\|_* + \lambda\|S\|_1 \quad \text{s.t.} \;\; X = L + S \tag{3}$$

Where $\|L\|_*$ denotes the tensor nuclear norm of 3D tensors, $\|S\|_1$ is the sum of absolute values of all the entries in S and λ is the regularization parameter (Lu et. al, 2019). They show that (3) can recover low rank and sparse components under certain conditions (when L_0 is not too large and $\mathcal{E}_0$ is reasonably sparse).

For the GPR image case, after the decomposition of X, the low rank component L corresponds to clutter part and sparse component $\mathcal{E}$ corresponds to target part.

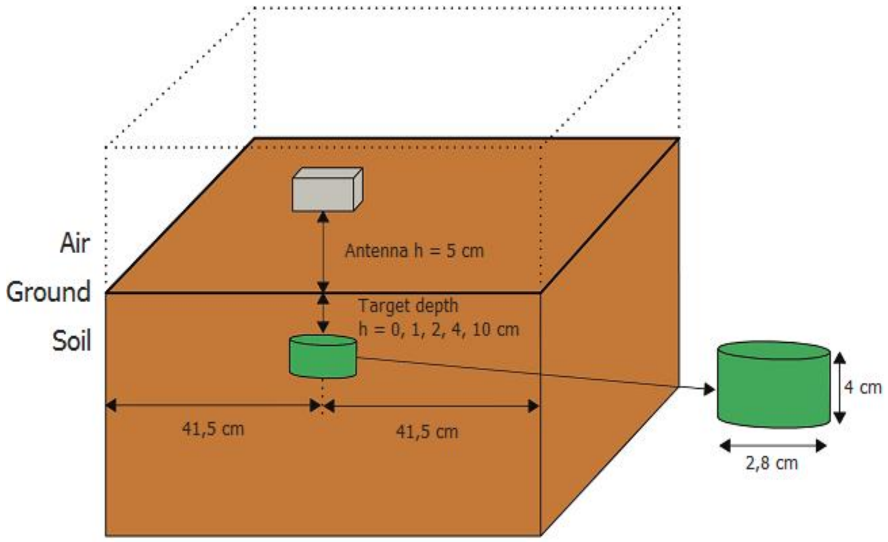

Figure 1. The experimental design of the simulated dataset.

3. EXPERIMENTAL RESULTS

The proposed TRPCA method is compared with the classical PCA (Abujarad & Omar, 2006) and recent RPCA method (Song et al., 2017). The obtained results show the superiority of our proposed method. The methods are evaluated both visually and quantitatively over the simulated dataset which is generated by the gprMax electromagnetic simulation software (Warren, Giannopoulos, & Giannakis, 2016). The experimental setup of the simulated dataset is shown in Figure 1. Our dataset contains, 2 different materials, 5 different burial depths and 6 different soil types. Since, they are constructed by simulation software, we have the reference images. These images give us ability to evaluate the performance of methods quantitatively which may not possible for the real datasets. The peak signal-to-noise ratio (PSNR) is used for the quantitative evaluation and the formulation is

$$\mathrm{PSNR(dB)} = 10\log\left(\frac{1}{\mathrm{MSE}}\right) \quad \textbf{(4)}$$

$$\mathrm{MSE} = \frac{1}{M \times N}\sum_{i=1}^{M}\sum_{j=1}^{N}(\mathrm{X_T}(i,j) - \mathrm{X_R}(i,j))^2 \quad \textbf{(5)}$$

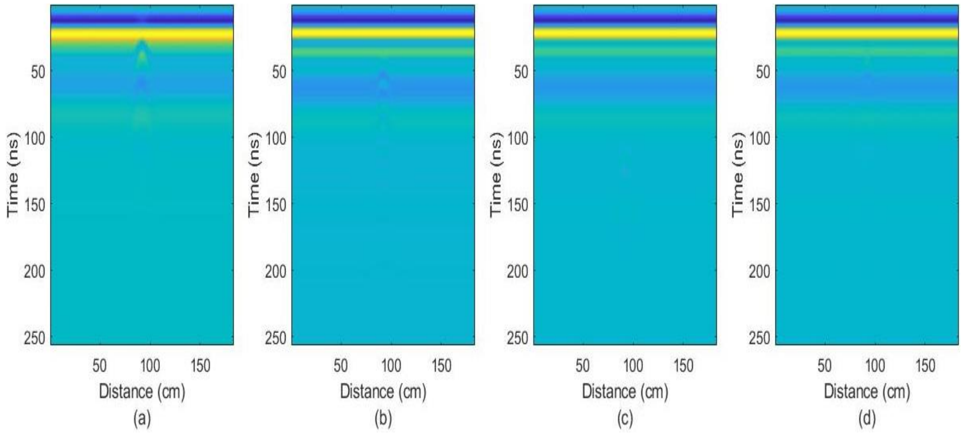

Figure 2. Raw data used for visual results: a) aluminum target, 1 cm burial depth and dry sand soil, b) aluminum target, 2 cm burial depth and wet sand soil, c) plastic target, 10 cm burial depth and dry clay soil, d) plastic target, 2 cm burial depth, dry loam soil.

MSE denotes the mean square error, X_T and X_R denote the obtained target component and reference GPR image, *i* and *j* are the pixel locations.

During the implementation of the methods, the following parameters are used:

- There is no parameter for the PCA,
- Penalization parameter $\lambda = 1.9e^{-2}$ is selected for RPCA and other parameters are default.
- Penalization parameter $\lambda = 6e^{-3}$ is selected for TRPCA, the patch size is selected as $r = 16$ and other parameters are default.

For the visual and quantitative performance evaluation part, four different scenarios are used and the experimental setup is presented in Figure 1. The sample GRP images from each case are shown in Figure 2. As seen in the Figure 2(a), the buried object is very closer to the surface and it is overlapped with clutter which is one of the challenging situations. In Figure 2(b), the buried target is aluminum and the soil is wet sand thus, its target signature is much weaker than the dry sand case in Figure 2(a). Figure 2(c) and (d) are plastic buried target and they are barely seen visually.

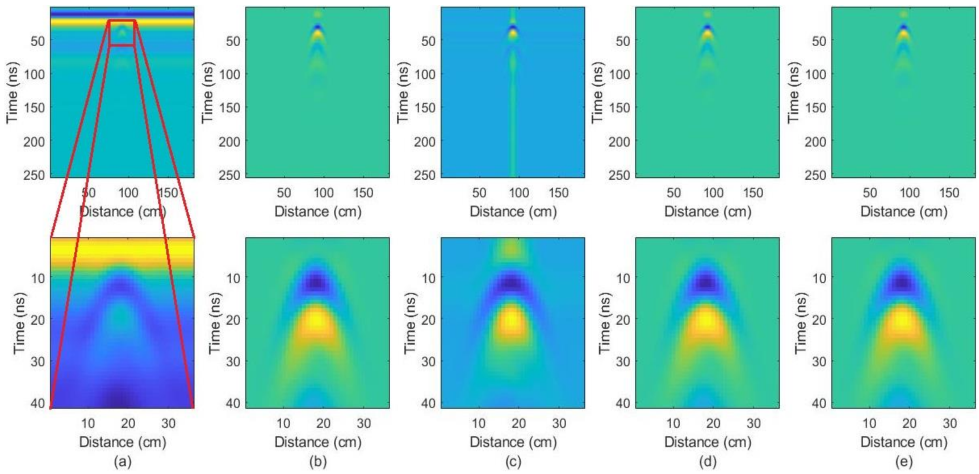

Figure 3. First Row: Original Results, Second Row: Zoomed Version: a) raw data, b) reference data clutter suppression results for, c) PCA, d) RPCA, e) TRPCA.

The visual results of the raw data in Figure 2(a) are presented in Figure 3(c)-(e) and the second row is the zoomed area for the target signature. As seen in the visual results, PCA cannot suppress the clutter since the target burial depth is 1 cm which is very shallow for PCA. The visual results of RPCA and TRPCA is similar however there is slight distortion around target signature in RPCA. The visual result of TRPCA looks identical to reference image and show better performance compared to the PCA and RPCA. The quantitative results support our visual results. As seen in the Table 1:

Table 1. PSNR (dB) results for aluminum target with different burial depths.

Aluminum Target	**PCA**	**RPCA**	**TRPCA**
0 cm	51.98	79.38	**80.26**
1 cm	36.22	130.35	**147.00**
2 cm	90.53	137.62	**144.28**
4 cm	97.27	146.78	**156.76**
10 cm	84.44	140.43	**145.78**

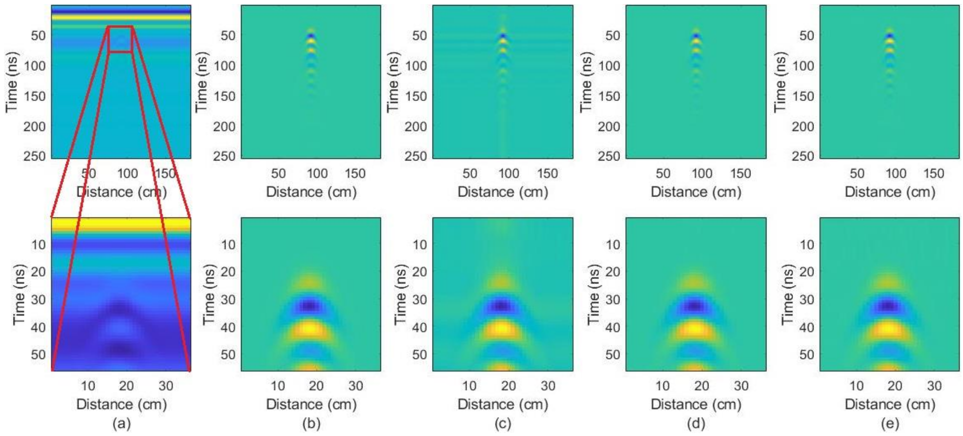

Figure 4. First Row: Original Results, Second Row: Zoomed Version: a) raw data, b) reference data clutter suppression results for, c) PCA, d) RPCA, e) TRPCA.

For all the burial depth TRPCA outperforms PCA and RPCA for aluminum target. Especially for the shallowly buried target (1 cm), TRPCA performance is approximately %13 better than the RPCA.

The visual results of the raw data in Figure 2(b) are presented in Figure 4(c)-(e) and the second row is the zoomed area for the target signature. As seen in the visual results, PCA obtains target signature however the residual of clutter is still available in the form of horizontal lines. The visual results of RPCA and TRPCA look similar however there is slight distortion around target signature in RPCA.

The visual result of TRPCA looks identical to reference image and show better performance compared to the PCA and RPCA.

The quantitative results support our visual results. As seen in the Table 2, for all the soil types TRPCA outperforms PCA and RPCA for aluminum target. Especially for the wet sand oil, TRPCA performance is approximately %10 better than the RPCA.

Table 2. PSNR (dB) results for aluminum target with different soil types.

Aluminum Target	**PCA**	**RPCA**	**TRPCA**
Dry sand soil	90.53	137.62	**144.28**
Damp sand soil	103.53	132.68	**137.03**
Wet sand soil	73.32	132.83	**145.82**
Dry clay soil	101.55	129.30	**135.48**
Wet clay soil	90.62	135.69	**141.32**
Dry loam soil	100.89	128.08	**135.69**

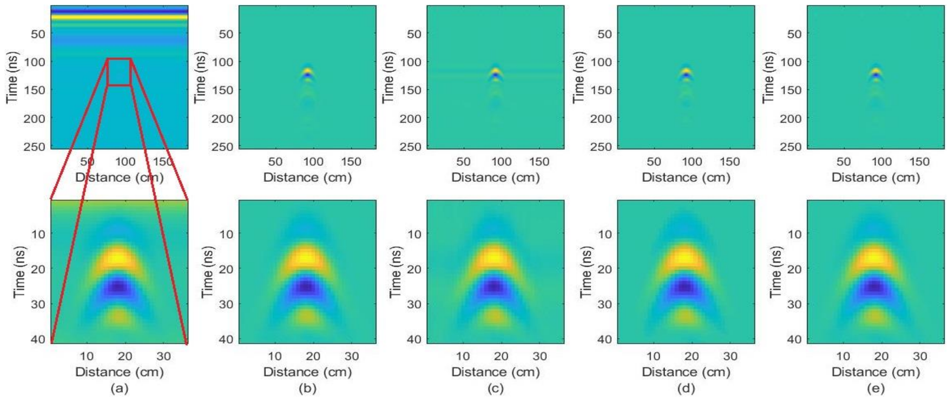

Figure 5. First Row: Original Results, Second Row: Zoomed Version: a) raw data, b) reference data clutter suppression results for, c) PCA, d) RPCA, e) TRPCA.

The visual results of the raw data in Figure 2(c) are presented in Figure 5(c)-(e) and the second row is the zoomed area for the target signature. As seen in the visual results, PCA obtains target signature however the residual of clutter is still available in the form of horizontal lines. The visual results of RPCA and TRPCA look similar to each other.

The quantitative results in plastic target case are not obvious as in the aluminum target. However, TRPCA outperform RPCA for 3 out of 5 GPR images. There are not dramatic differences between TRPCA and PRCA in the sense of PSNR (dB) value. Both of them outperform the classical PCA method with huge differences in quantitative analysis.

Table 3. PSNR (dB) results for plastic target with different burial depths.

Plastic Target	PCA	RPCA	TRPCA
0 cm	53.91	**92.95**	80.26
1 cm	58.71	101.90	**104.59**
2 cm	99.82	126.04	**128.60**
4 cm	104.11	**132.06**	130.85
10 cm	96.55	115.36	**125.79**

The visual results of the raw data in Figure 2(d) are presented in Figure 6(c)-(e) and the second row is the zoomed area for the target signature. As seen in the visual results, PCA obtains target signature however the residual of clutter is still available in the form of horizontal lines. The visual results of RPCA and TRPCA look similar to each other. Both of them effectively suppressed the clutter and outperform the classical PCA method.

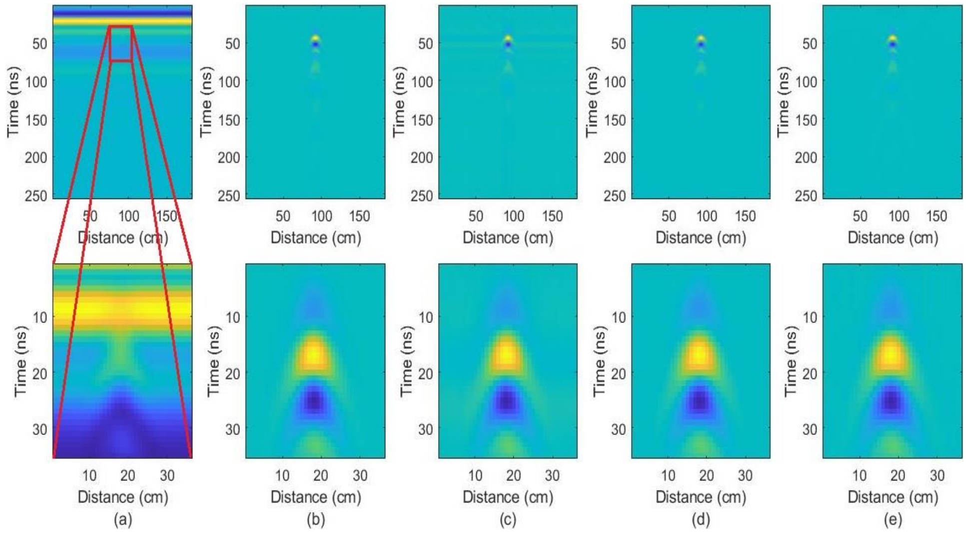

Figure 6. First Row: Original Results, Second Row: Zoomed Version: a) raw data, b) reference data clutter suppression results for, c) PCA, d) RPCA, e) TRPCA.

Again, the quantitative results in this case are not obvious as in the aluminum target. However, TRPCA outperform RPCA for 4 out of 6 GPR images. There are not dramatic differences between TRPCA and PRCA and both of them outperform the classical PCA method with huge differences.

Table 4. PSNR (dB) results for plastic target with different soil types.

Aluminum Target	**PCA**	**RPCA**	**TRPCA**
Dry sand soil	47.42	**72.46**	68.26
Damp sand soil	92.17	121.62	**126.99**
Wet sand soil	70.29	**135.67**	133.52
Dry clay soil	99.82	126.04	**128.60**
Wet clay soil	94.12	125.82	**131.11**
Dry loam soil	99.25	125.92	**128.87**

4. CONCLUSION

The proposed TRPCA based clutter suppression method applies a novel pre-transformation step during the construction of image-patch tensor in GPR. The 1D A-scans are converted to 2D images and they are concatenated to construct multi-dimensional image tensor. Since, 2D GPR images are formed by the concatenation of A-scans, the constructed new image tensor from A-scans are interrelated. Then, TRPCA method is used for the decomposition of the constructed GPR image tensor. The obtained results are compared with the classical PCA and recently proposed RPCA method over the simulation dataset both visually and quantitatively. The obtained results show that TRPCA method heavily outperforms classical PCA and recently proposed RPCA in the aluminum target case and it has better decomposition results in the plastic target case.

REFERENCES

Abujarad, F., and Omar, A. (2006). “GPR Data Processing Using the Component-Separation Methods PCA and ICA”. *Proceedings of the IEEE International Workshop on Imagining Systems and Techniques (IST 2006)*, 60-64. doi:10.1109/IST.2006.1650776.

Candès, E. J., Li, X., Ma, Y., and Wright, J. (2011). “Robust Principal Component Analysis?”. *Journal of the ACM*, 58(3), 1-37. doi:10.1145/1970392.1970395.

Daniels, D. J. (2005). “Ground Penetrating Radar”. *Encyclopedia of RF and Microwave Engineering*, John Wiley & Sons.

Kumlu, D., and Erer, I. (2018). “The Multiscale Directional Neighborhood Filter and its Application to Clutter Removal in GPR Data”. *Signal, Image and Video Processing (SIViP)*, 12(7), 1237-1244.

Kumlu, D., and Erer, I. (2019a). “Clutter Removal Techniques in Ground Penetrating Radar for Landmine Detection: A Survey”. In H. Tozan and M. Karatas (Eds.), *Operations Research for Military Organizations* (pp. 375-399). Hershey, PA: IGI Global.

Kumlu, D., and Erer, I. (2019b), “Improved Cutter Removal in GPR by Robust Nonnegative Matrix Factorization”. In *IEEE Geoscience and Remote Sensing Letters*, 17(6), 958-962. Retrieved from https://ieeexplore.ieee.org/stamp/stamp.jsp?arnumber=8836507

Kumlu, D., and Erer, I. (2020a). “GPR Clutter Reduction by Robust Orthonormal Subspace Learning”. In *IEEE Access*, Vol. 8, 74145-74156. Retrieved from https://ieeexplore.ieee.org/stamp/stamp.jsp?arnumber=9069272

Kumlu, D., Erer, I., and Kaplan, N.H., (2020b). “Low Complexity Clutter Removal in GPR Images via Lattice Filters”, *Digital Signal Processing*, Vol. 101, 102724. doi:10.1016/j.dsp.2020.102724.

Lu, C., Feng, J., Chen, Y., Liu, W., Lin, Z., and Yan, S. (2019). "Tensor Robust Principal Component Analysis with a New Tensor Nuclear Norm". *IEEE Transactions on Pattern Analysis and Machine Intelligence*, 42(4), 925-938. doi:10.1109/tpami.2019.2891760.

Song, X., Xiang, D., Zhou, K., and Su, Y. (2017). "Improving RPCA-based Clutter Suppression in GPR Detection of Antipersonnel Mines", *IEEE Geoscience and Remote Sensing Letters*, 14(8), 1338-1342. Retrieved from https://ieeexplore.ieee.org/stamp/stamp.jsp?tp=&arnumber=7970124

Song, X., Liu, T., Xiang, D., and Su, Y. (2019). "GPR Antipersonnel Mine Detection Based on Tensor Robust Principal Analysis". *Remote Sensing*, 11(8), 984.doi:10.3390/rs11080984.

Tivive, F. H. C., Bouzerdoum, A., and Abeynayake, C. (2019). "GPR Target Detection by Joint Sparse and Low-Rank Matrix Decomposition". IEEE Transactions on Geoscience and Remote Sensing, 57(5), 2583-2595. Retrieved from https://ieeexplore.ieee.org/stamp/stamp.jsp?tp=&arnumber=8522060

Verma, P. K., Gaikwad, A. N., Singh, D., and Nigam, M. J. (2009). "Analysis of Clutter Reduction Techniques for through Wall Imaging in UWB Range". *Progress In Electromagnetics Research*, Vol. 17, 29-48. Retrieved from http://www.jpier.org/PIERB/pierb17/03.09060903.pdf

Warren, C., Giannopoulos, A., and Giannakis, I. (2016). "gprMax: Open Source Software to Simulate Electromagnetic Wave Propagation for Ground Penetrating Radar". *Computer Physics Communications*, Vol. 209, 163-170. doi:10.1016/j.cpc.2016.08.020.

Wold, S., Esbensen, K., and Geladi, P. (1987). "Principal Component Analysis". *Chemometrics and Intelligent Laboratory Systems*, 2(1-3), 37-52. doi:10.1016/0169-7439(87)80084-9.